Sigma J Eng & Nat Sci 36 (4), 2018, 935-950

Sigma Journal of Engineering and Natural Sciences
Sigma Mühendislik ve Fen Bilimleri Dergisi

Research Article

EARTQUAKE BEHAVIOUR OF THICK PLATES RESTING ON ELASTIC FOUNDATION WITH FIRST ORDER FINITE ELEMENT

Yaprak Itır ÖZDEMİR*

Department of Civil Engineering, Karadeniz Technical University, TRABZON; ORCID:0000-0002-0658-1366

Received: 08.12.2017 Revised: 27.03.2018 Accepted: 09.04.2018

ABSTRACT

This paper focus on to study dynamic analysis of thick plates resting on Winkler foundation. The governing equation is derived from Mindlin's theory. This study is a parametric analysis therefore, the effects of the thickness/span ratio, the aspect ratio and the boundary conditions on the linear responses of thick plates subjected to earthquake excitations is studied. In the analysis, as a dynamic solution the Newmark-β method is used for the time integration and finite element method is used for spatial integration. While using finite element method first order element is used. This element is 4-noded and it's formulation is derived by using first order displacement shape functions. A computer program using finite element method is coded in C++ to analyze the plates clamped or simply supported along all four edges. Graphs are presented that should help engineers in the design of thick plates subjected to earthquake excitations. It is concluded that 4-noded finite element can be effectively used in the earthquake analysis of thick plates. It is also concluded that, in general, the changes in the thickness/span ratio are more effective on the maximum responses considered in this study than the changes in the aspect ratio.

Keywords: Parametric forced vibration analysis, thick plate, mindlin's theory, first order finite element, winkler foundation.

1. INTRODUCTION

The plates resting on elastic foundation is one of the most popular topics for the last decade in many engineering application. Winkler model, Pasternak model, Hetenyi model, Vlasov and Leont'ev model are the models used by the researchers to calculate the soil effects on the plate.

Winkler model is used as a set of uncorrelated elastic springs attached to each node of the plate [1]. In this method, the deflections are only related with the load on the plate. The deflection of neighbouring points of the foundation is independent of each other. Hetenyi [2] proposed a two-parameter model, Pasternak model takes in to account the effects of shear interaction among joining points in the foundation [3]. Vlasov and Leont'ev [4] related the solution with a γ parameter which is calculated with soil material and thickness of the soil.

The dynamic behavior of thick elastic plates has been investigated by many researchers [5-15]. Ayvaz et all. [19] derived the equations of motions for thick orthotropic elastic plates using Hamilton's principle, but did not present any results. Omurtag and Kadıoğlu [20] are studied free vibration analysis of orthotropic plates resting on Pasternak foundation by mixed finite element

* Corresponding Author: e-mail: yaprakozdemir@hotmail.com, tel: (462) 377 40 18

formulation, Ayvaz Y. and Oguzha n C.B. [21] are analysis free vibration of thick plates resting on Vlasov elastic foundation. Ozgan and Daloğlu [22] are analysis free vibration of thick plates resting on Winkler elastic foundation. All these studies are use 4- and 8- noded finite element which are second and third ordered mathematically. These elements are known having shear locking problem. Thick plates have a shear locking problem [23] while the thickness becomes smaller. This means that the bending energy, which should dominate the shear terms, will be incorrectly estimated to be zero in thin plate problems. Shear locking can be avoided by increasing the mesh size, i.e. using finer mesh, but if the thickness/span ratio is "too small", convergence may not be achieved even if the finer mesh is used for the first and second order displacement shape functions. Either refining the finite-element mesh or increasing the order of the shape functions can improve the accuracy of finite-element solutions. The former is called h-version and the latter p-version. It is well known that p convergence is more rapid than h convergence using the same number of degrees of freedom (DOFs) [24]. These problems can be prevented with using true shape function while built up the mathematical model. The author formed a new 17 noded, 4 order shape function finite element at the past studies and this element is free from shear locking [25] and also author used this element for thick plates resting on Winkler foundation [26]. This element is a new element and neither free vibration nor forced vibration analysis of thick plates resting on Winkler foundation is used before.

The purpose of this paper is to parametric earthquake analysis of thick plates resting on Winkler foundation, to determine the effects of the thickness/span ratio, the aspect ratio and the boundary conditions on the linear responses of the thick plates subjected to earthquake excitations. A computer program using finite element method is coded in C++ to analyse the plates clamped or simply supported along all four edges. In the program, the finite element method is used for spatial integration and the Newmark-β method is used for the time integration. Finite element formulation of the equations of the thick plate theory is derived by using first order displacement shape functions. In the analysis, 4-noded finite element is used to construct the stiffness and mass matrices since shear locking problem does not occur if this element is used in the finite element modelling of the thick plates [27].

2. MATHEMATICAL MODEL

The governing equation for a flexural plate (Fig. 1) subjected to an earthquake excitation without damping can be given as [16, 28]

$$[M]\{\ddot{w}\}+[K]\{w\}=[F]=-[M]\{\ddot{u}_g\} \tag{1}$$

where [K] and [M] are the stiffness matrix and the mass matrix of the plate, respectively, w and $\ddot{w}$ are the lateral displacement and the second derivative of the lateral displacement of the plate with respect to time, respectively, $\ddot{u}_g$ is the earthquake acceleration.

In order to do forced vibration analysis of a plate, the stiffness, [K], mass matrices, [M], and equivalent nodal loads vector, [F], of the plate should be constructed. The evaluation of these matrices is given in the following sections.

The total strain energy of plate-soil-structure system (see Fig. 1) can be written as;

$$\Pi= \Pi_p+ \Pi_s+ V \tag{2}$$

where Πp is the strain energy in the plate,

$$\Pi_p = \frac{1}{2}\int_A \left(-\frac{\partial\varphi_x}{\partial x} \quad \frac{\partial\varphi_y}{\partial y} \quad -\frac{\partial\varphi_x}{\partial y}+\frac{\partial\varphi_y}{\partial x}\right)^T E_\kappa \left(-\frac{\partial\varphi_x}{\partial x} \quad \frac{\partial\varphi_y}{\partial y} \quad -\frac{\partial\varphi_x}{\partial y}+\frac{\partial\varphi_y}{\partial x}\right) d_A +$$

$$\frac{k}{2}\int_A \left(-\varphi_x+\frac{\partial w}{\partial x} \quad \varphi_y+\frac{\partial w}{\partial y}\right)^T E_\gamma \left(-\varphi_x+\frac{\partial w}{\partial x} \quad \varphi_y+\frac{\partial w}{\partial y}\right) d_A - \tag{3}$$

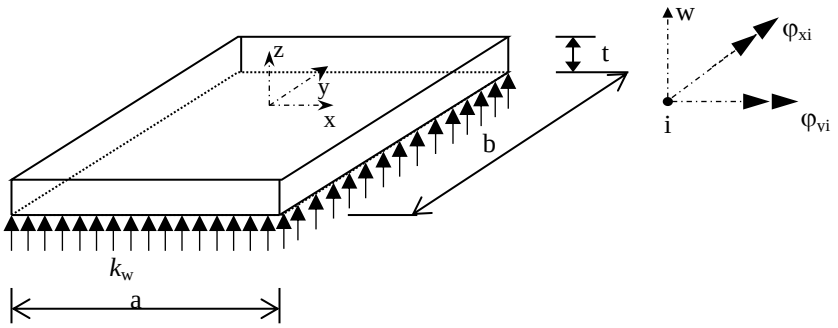

Figure 1. T he sample plate used in this study

where Πs is the strain energy stored in the soil,

$$\Pi_s = \frac{1}{2}\int_0^H \int_{-\infty}^{\infty} \int_{-\infty}^{\infty} \sigma_{ij}\varepsilon_{ij} \tag{4}$$

and V is the potential energy of the earthquake loading;

$$V = -\int_A \bar{q} w d_A \tag{5}$$

In this equation E_κ and E_γ are the elasticity matrix and these matrices are given below at Eq. (14), $\bar{q}$ shows earthquake loading.

2.1. Evaluation of the Stiffness Matrix

The total strain energy of the plate-soil system according to Eq. (2) is;

$$U = \frac{1}{2}\int_A \left(-\frac{\partial\varphi_x}{\partial x} \quad \frac{\partial\varphi_y}{\partial y} \quad -\frac{\partial\varphi_x}{\partial y}+\frac{\partial\varphi_y}{\partial x}\right)^T E_\kappa \left(-\frac{\partial\varphi_x}{\partial x} \quad \frac{\partial\varphi_y}{\partial y} \quad -\frac{\partial\varphi_x}{\partial y}+\frac{\partial\varphi_y}{\partial x}\right) d_A +$$

$$\frac{k}{2}\int_A \left(-\varphi_x+\frac{\partial w}{\partial x} \quad \varphi_y+\frac{\partial w}{\partial y}\right)^T E_\gamma \left(-\varphi_x+\frac{\partial w}{\partial x} \quad \varphi_y+\frac{\partial w}{\partial y}\right) d_A +$$

$$\frac{1}{2}\int_A \left(w_{x,y}\right)^T K \left(w_{x,y}\right) d_A \tag{6}$$

At this equation the first and second part gives the conventional element stiffness matrix of the plate, $[k_p^e]$, differentiation of the third integral with respect to the nodal parameters yields a matrix, $[k_w^e]$, which accounts for the axial strain effect in the soil. Thus the total energy of the plate-soil system can be written as;

$$U_e = \frac{1}{2}\{w_e\}^T \left(\left[k_p^e\right] + \left[k_w^e\right] \right) \{w_e\} d_A \tag{7}$$

where

$$\{w_e\} = \left[w_1 \quad \varphi_{y1} \quad \varphi_{x1} \quad \dots \quad w_n \quad \varphi_{yn} \quad \varphi_{xn} \right]^T \tag{8}$$

Assuming that in the plate of Fig. 1 u and v are proportional to z and that w is the independent of z [29], one can write the plate displacement at an arbitrary x, y, z in terms of the two slopes and a displacement as follows;

$$\{w, v, u\} = \{w_{0(x,y,t)}, -z\varphi_{y\,(x,y,t)}, z\varphi_{x\,(x,y,t)}\} \tag{9}$$

where w_0 is average displacement of the plate, and φ_x and φ_y are the bending slopes in the x and y directions, respectively.

The nodal displacements for 4-noded quadrilateral serendipity element (MT4) (Fig. 2) can be written as follows;

$$w = \sum_1^{17} h_i w_i \,,\; v = -z\varphi_y = z\sum_1^{17} h_i \varphi_{yi} \,,\; u = -z\varphi_x = z\sum_1^{17} h_i \varphi_{xi} \qquad , \quad (i=1, 2, 3, 4) \tag{10}$$

The displacement function chosen for this element is;

$$w = c_1 + c_2 r + c_3 s + c_4 rs \tag{11}$$

From this assumption, it is possible to derive the displacement shape function to be;

$$hi = [h_1, h_2, h_3, h_4] \tag{12}$$

where

$$h_1 = (0.25)*(1+r)*(1+s), \qquad h_2 = (0.25)*(1-r)*(1+s),$$
$$h_3 = (0.25)*(1-r)*(1-s), \qquad h_4 = (0.25)*(1+r)*(1-s), \tag{13}$$

The 3x3 Jacobian matrix required in this formulation is;

$$J = \begin{bmatrix} 1 & 0 & 0 \\ 0 & y_s & x_s \\ 0 & y_r & x_r \end{bmatrix} \tag{14}$$

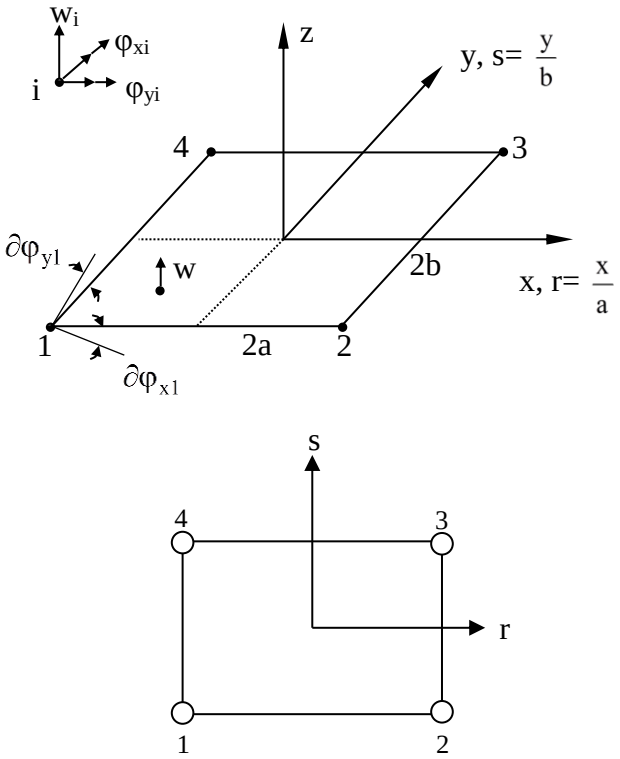

Figure 2. 4-noded (first order) quadrilateral finite element used in this study [31].

Where

$$x_r = \sum_{i=1}^{4}\left(h_{i,r}x_i\right).....y_r = \sum_{i=1}^{4}\left(h_{i,r}y_i\right)$$

$$x_s = \sum_{i=1}^{4}\left(h_{i,s}x_i\right).....y_s = \sum_{i=1}^{4}\left(h_{i,s}y_i\right) \quad , \tag{15}$$

The inverse of J becomes

$$J^{-1} = \begin{bmatrix} 1 & 0 & 0 \\ 0 & s_y & r_y \\ 0 & s_x & r_x \end{bmatrix} \tag{16}$$

We need certain derivatives with respect to local coordinates, which are placed into a 3x3 matrix;

$$\begin{bmatrix} w_z & v_z & u_z \\ w_s & v_s & u_s \\ w_r & v_r & u_r \end{bmatrix} = \sum_{i=1}^{4} \begin{bmatrix} 0 & -f_i\varphi_{yi} & f_i\varphi_{xi} \\ f_{i,s}w_i & -zf_{i,s}\varphi_{yi} & zf_{i,s}\varphi_{xi} \\ f_{i,r}w_i & -zf_{i,r}\varphi_{yi} & zf_{i,r}\varphi_{xi} \end{bmatrix} \tag{17}$$

Transformation of these derivatives to global coordinates is accomplished using the inverse of the Jacobian matrix, as follows;

$$\begin{bmatrix} w_z & v_z & u_z \\ w_y & v_y & u_y \\ w_x & v_x & u_x \end{bmatrix} = J^{-1} \begin{bmatrix} w_z & v_z & u_z \\ w_s & v_s & u_s \\ w_r & v_r & u_r \end{bmatrix} \tag{18}$$

The five types of nonzero strains to be considered for this element are;

$$\varepsilon = \begin{bmatrix} \varepsilon_x \\ \varepsilon_y \\ \gamma_{xy} \\ \gamma_{xz} \\ \gamma_{yz} \end{bmatrix} = \begin{bmatrix} u_x \\ v_y \\ u_y + v_x \\ u_z + w_x \\ v_z + w_y \end{bmatrix} \tag{19}$$

As a preliminary matter before formulating element stiffness matrix, matrix B partitioned and z factored from the upper part, as follows [30].;

$$B = \begin{bmatrix} B_k \\ B_\gamma \end{bmatrix} = \begin{bmatrix} z\overline{B}_k \\ B_\gamma \end{bmatrix} \tag{20}$$

where B_k has three rows and B_γ has two rows, then the stiffness matrix for this element is written as;

$$K = \int_V B^T E B dV = \int_V \begin{bmatrix} z\overline{B}_k^T & B_\gamma^T \end{bmatrix} \begin{bmatrix} E_k & 0 \\ 0 & E_\gamma \end{bmatrix} \begin{bmatrix} z\overline{B}_k^T \\ B_\gamma^T \end{bmatrix} dV$$

$$K = \int_V \left(z^2 \overline{B}_k^T E_k \overline{B}_k \right) + \left(\overline{B}_\gamma^T E_\gamma \overline{B}_\gamma \right) dV \tag{21}$$

Integration through the thickness yields;

$$K = \int_A \left(\overline{B}_k^T \overline{E}_k \overline{B}_k + \overline{B}_\gamma^T \overline{E}_\gamma \overline{B}_\gamma \right) dA \tag{22}$$

Thus,

$$K = \int_A \overline{B}^T \overline{E} \overline{B} dA = \int_{-1}^{1} \int_{-1}^{1} \overline{B}^T \overline{E} \overline{B} |J| dr ds \tag{23}$$

which must be evaluated numerically [30].

Thus this is a plane stress problem equation, [$\overline{E}_k$] is of size 3x3 and [$\overline{E}_\gamma$] is of size 2x2 and they can be written as follows [31, 32]:

$$[\overline{E}_k]=\frac{t^3}{12}\begin{bmatrix} \frac{E}{(1-\nu^2)} & \frac{\nu E}{(1-\nu^2)} & 0 \\ \frac{\nu E}{(1-\nu^2)} & \frac{E}{(1-\nu^2)} & 0 \\ 0 & 0 & \frac{E}{2(1-\nu)} \end{bmatrix};\ [\overline{E}_\gamma]=k\,t\begin{bmatrix} \frac{E}{2.4(1+\nu)} & 0 \\ 0 & \frac{E}{2.4(1+\nu)} \end{bmatrix} \tag{24}$$

where E, υ, and t are modulus of the elasticity, Poisson's ratio, and the thickness of the plate, respectively, k is a constant to account for the actual non-uniformity of the shearing stresses. By assembling the element stiffness matrices obtained, the system stiffness matrix is obtained.

2.2. Foundation formulation

As explained before, Winkler model is the simplest model for the plates resting on elastic foundation. In this model, all the deflections on the plate are due to the load on it. The foundation is represented with a set of uncorrelated elastic springs. So in the analysis, the stiffness of these springs are calculated and are added to the element stiffness matrix. The stiffness matrices for the Winkler foundation can be derived by;

$$k_w = k\int_{-1}^{1}\int_{-1}^{1}[h]^T[h]J|drds\,. \tag{25}$$

where *k* is the elastic foundation modulus.

After calculating all element stiffness matrices, global stiffness matrix can be assembled as;

$$[K]=\sum_{i=1}^{p_e}\left([k_p]+[k_w]\right) \tag{26}$$

where p_e is the node number.

2.3. Evaluation of the mass matrix

The formula for the consistent mass matrix of the plate may be written as

$$M=\int_{\Omega} H_i^T \mu H_i d\Omega\,. \tag{27}$$

In this equation, μ is the mass density matrix of the form [32]

$$\mu=\begin{bmatrix} m_1 & 0 & 0 \\ 0 & m_2 & 0 \\ 0 & 0 & m_3 \end{bmatrix}, \tag{28}$$

where $m_1=\rho_p t$, $m_2=m_3=\frac{1}{12}\left(\rho_p t^3\right)$, and ρ_p is the mass densities of the plate. and H_i can be written as follows,

$$H_i = \left[h_i \quad dh_i / dy \quad dh_i / dx \right] \qquad i = 1 \ldots 4. \tag{29}$$

It should be noted that the rotation inertia terms are not taken into account. By assembling the element mass matrices obtained, the system mass matrix is obtained.

2.4. Evaluation of equivalent nodal loads vector

Equivalent nodal loads, [F], can be obtained by the following equation.

$$[F] = \int H_i^T \bar{q} \, d\Omega . \tag{30}$$

In this equation, H_i can be obtained by Equation (29), and $\bar{q}$ denotes

$$-[M]\{\ddot{u}_g\} \tag{31}$$

It should also be noted that, the Newmark-β method is used for the time integration of Equation (1) by using the average acceleration method.

3. NUMERICAL EXAMPLES

3.1. Data for numerical examples

In the light of the results given in references [25, 27], the aspect ratios, b/a, of the plate are taken to be 1, 2.0, and 3.0. The thickness/span ratios, t/a, are taken as 0.05, 0.1, 0.2, and 0.3 for each aspect ratio. The shorter span length of the plate is kept constant to be 3 m. The mass density, Poisson's ratio, and the modulus of elasticity of the plate are taken to be 2.5 kN s^2/m^2, 0.2, and 2.7×10^7 kN/m^2. Shear factor k is taken to be 5/6. The subgrade reaction modulus of the Winkler-type foundation is taken to be 5000 kN/m^3.

In order to obtain the response of each plate by using the time history analysis, the East-West component of March 13 1992 Erzincan earthquake in Turkey is used. East-West component of earthquake is applied vertically direction to the plate. Duration of this earthquake is 21 s, but, in this study, the first 8 s of the earthquake is used since the peak value of the record occurred in this range (Fig. 3).

For the sake of accuracy in the results, rather than starting with a set of a finite element mesh size and time increment, the mesh size and time increment required to obtain the desired accuracy were determined before presenting any results. This analysis was performed separately for the mesh size and time increment. It was concluded that the results have acceptable error when equally spaced 20x20 mesh sizes are used for a 3 m x 3 m plate even if it is a thin plate, if the 0.01s time increment is used. Length of the elements in the x and y directions are kept constant for different aspect ratios as in the case of square plate.

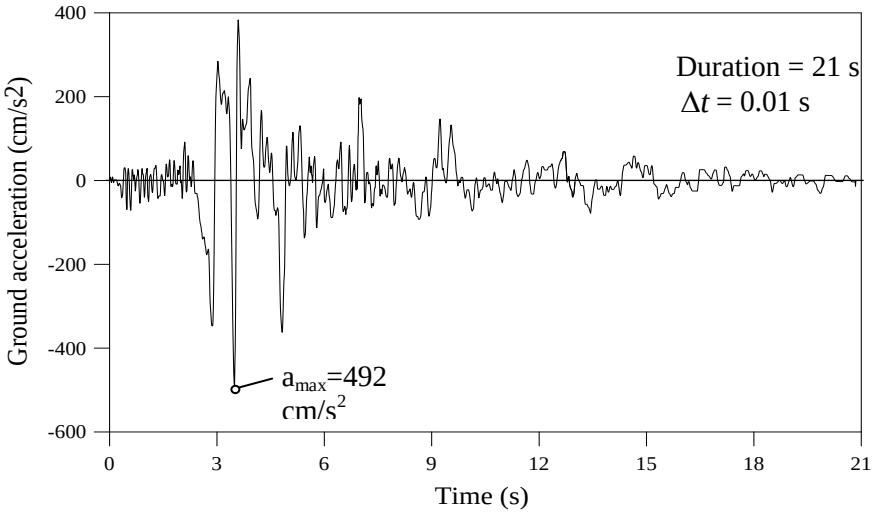

Figure 3. East-West component of the March 13, 1992 Erzincan earthquake in Turkey .

3.2. Results

One of the purposes of this paper was to determine the time histories of the displacements and the bending moments at different points of the thick and thin plates subjected to earthquake excitations, but presentation of all of the time histories would take up excessive space. Hence, only the absolute maximum displacements and bending moments for different thickness/span ratio and aspect ratio are presented after two time histories are given. This simplification of presenting only the maximum responses is supported by the fact that the maximum values of these quantities are the most important ones for design. These results are presented in graphical rather than in tabular form.

The time histories of the center displacements of the thick clamped plates resting on elastic foundation with the subgrade reaction modulus of the Winkler-type foundation 5000 kN/m3 for b/a= 1.0, and 2.0 when t/a=0.2 are given in Figs. 4(a), and 4(b), respectively.

As seen from Figs. 4(a), and 4(b), the center displacements of the thick simply supported plates for b/a = 1, and t/a = 0.05, and for b/a = 2, and t/a = 0.05, reached their absolute maximum values of 0.06162 mm at 3.48 s, and of 0.14835 mm at 3.48 s, respectively. These absolute maximum values are different even with the same occurring time as the dynamic characteristics of the thick plates affect the response. It is also understandable that the system becomes more flexible as the aspect ratio increases.

The absolute maximum displacements of the thick and thin plates for different aspect ratios, and thickness/span ratios are given in Fig. 5 for the thick plates simply supported along all four edges and in Fig. 6 for the thick plates clamped along all four edges.

As seen from Figs. 5, and 6, the absolute maximum displacements of the thick plates increase with increasing aspect ratio for a constant t/a ratio. The same displacements decrease with increasing t/a ratio for a constant b/a ratio. As also seen from these figures, the decrease in the absolute maximum displacement for a constant b/a ratio increases with increasing b/a ratio. The curves for a constant value of the aspect ratio, b/a are fairly getting closer to each other as the value of t/a increases. This shows that the curves of the absolute maximum displacements will almost coincide with each other when the value of the thickness/span ratio, t/a, increases more. In other words, the increase in the thickness/span ratio will not affect the absolute maximum displacements after a determined value of t/a.

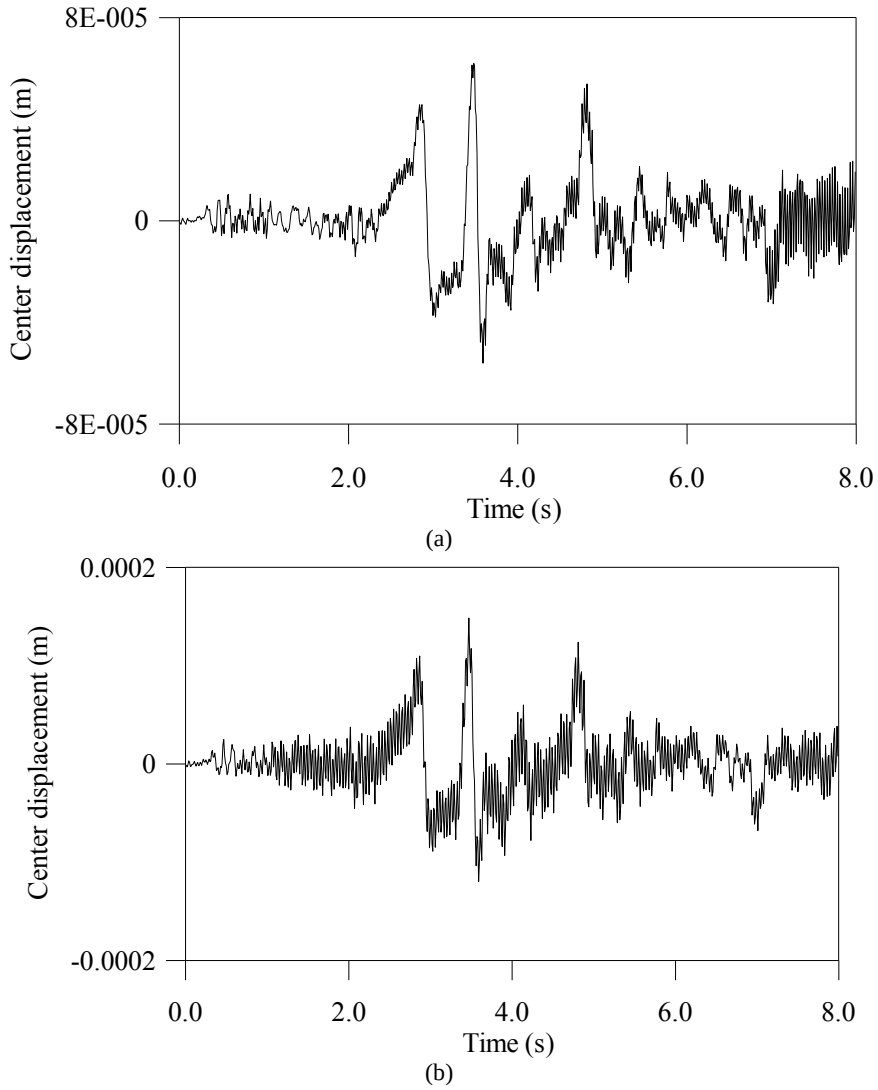

Figure 4. The time history of the center displacement of the thick simply supported plate resting on Winkler foundation for (a) b/a=1.0 and t/a=0.05, and (b) b/a=2.0 and t/a=0.05.

As also seen from Figs. 5, and 6, the absolute maximum displacements of the thick simply supported plates are larger than those of the thick clamped plates for the same aspect and thickness/span ratios. In general, the effects of the changes in the thickness/span ratios on the absolute maximum displacement are larger than the changes in the aspect ratios.

The absolute maximum bending moments M_x at the center of the thick plates for different aspect ratios and thickness/span ratios are given in Fig. 7 for the thick simply supported plates and in Fig. 8 for the thick clamped plates, respectively.

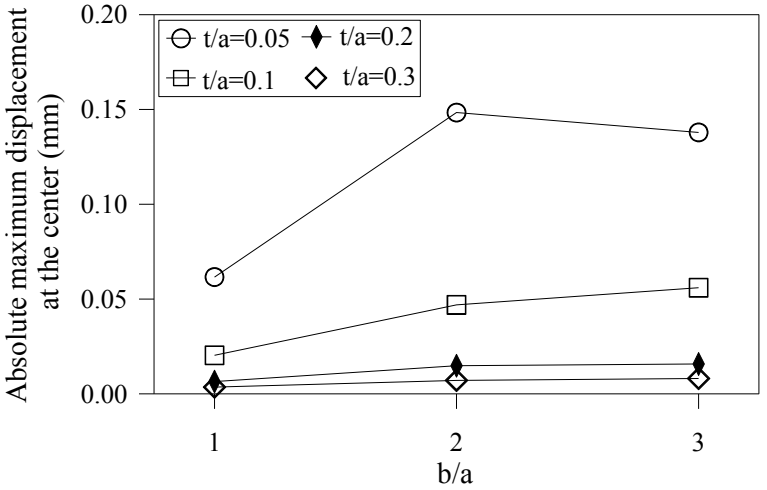

Figure 5. Absolute maximum displacement of the thick simply supported plates resting on Winkler foundation for different aspect ratios and thickness/span ratios.

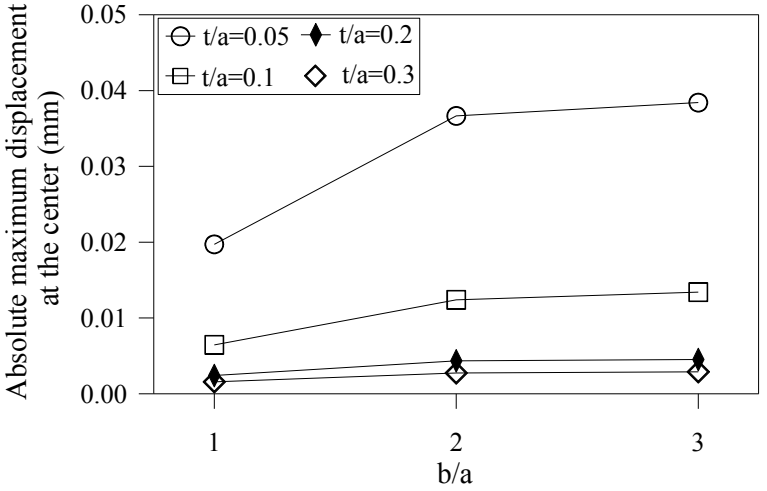

Figure 6. Absolute maximum displacement of the thick clamped plates resting on Winkler foundation for different aspect ratios and thickness/span ratios.

As seen from Fig. 7, the absolute maximum bending moment, M_x, at the center of the thick simply supported plates increases with increasing aspect ratio and thickness/span ratio. The increases in the absolute maximum bending moment, M_x, increase with increasing aspect and thickness/span ratios. This is understandable that increasing the aspect ratio makes the plate stiffer in the short span, the x axis, direction. As also seen from this figure, in general, the effects of the changes in the aspect ratios on the absolute maximum bending moment, M_x, are larger than the changes in the thickness/span ratios.

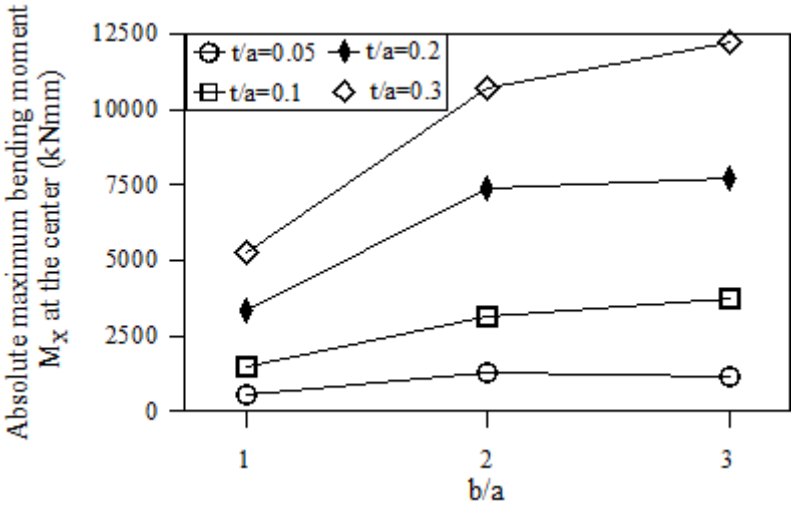

Figure 7. Absolute maximum bending moment M_x at the center of the thick simply supported plates resting on Winkler foundation for different aspect ratios and thickness/span ratios.

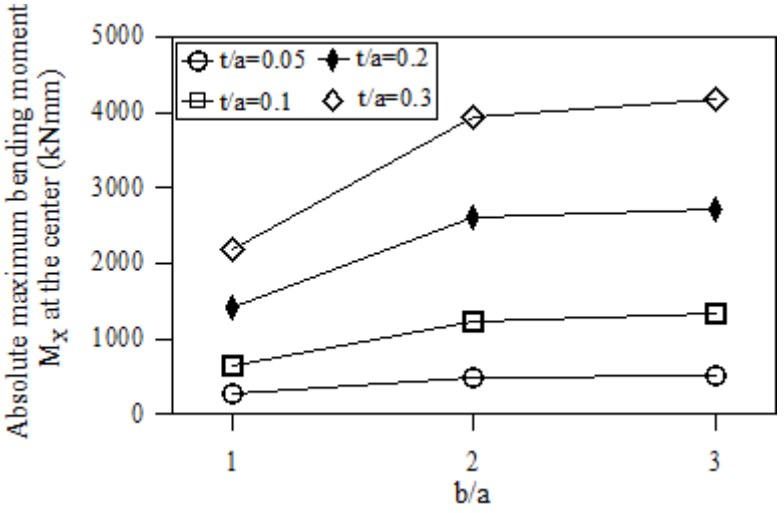

Figure 8. Absolute maximum bending moment M_x at the center of the thick clamped plates resting on Winkler foundation for different aspect ratios and thickness/span ratios.

As seen from Fig. 8, the absolute maximum bending moment, M_x, at the center of the thick clamped plates, as in the case of the absolute maximum bending moment, M_x, at the center of the thick simply supported plates, increases with increasing aspect ratio and thickness/span ratio. The increases in the absolute maximum bending moment, M_x, increase with increasing aspect and thickness/span ratios. This is also understandable that increasing the aspect ratio makes the plate stiffer in the short span, the x axis, direction. As also seen from this figure, in general, the effects of the changes in the aspect ratios on the absolute maximum bending moment, M_x, are larger than the changes in the thickness/span ratios.

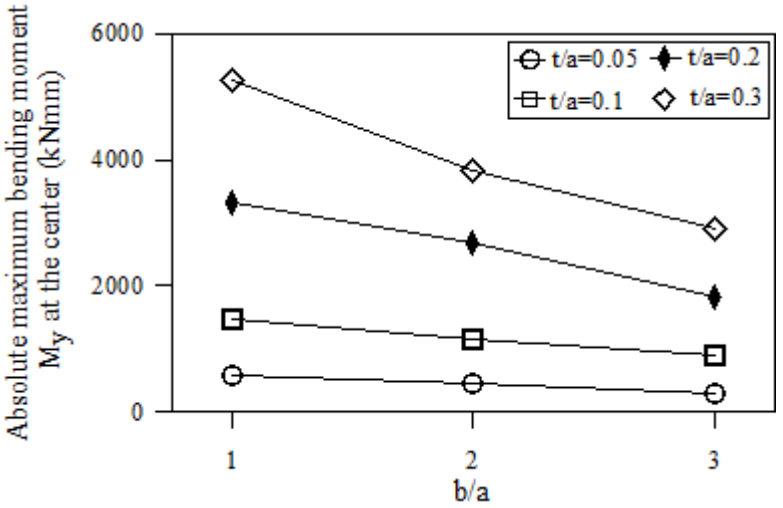

Figure 9. Absolute maximum bending moment M_y at the center of the thick simply supported plates resting on Winkler foundation for different aspect ratios and thickness/span ratios.

The absolute maximum bending moments M_y at the center of the thick plates for different aspect ratios and thickness/span ratios are given in Fig. 9 for the thick simply supported plates and in Fig. 10 for the thick and clamped plates, respectively.

As seen from Fig. 9, the absolute maximum bending moment, M_y, at the center of the thick simply supported plates decreases with increasing aspect ratio and increases with increasing thickness/span ratio. The decrease in the absolute maximum bending moment, M_y, increase with increasing aspect ratio. The increase in the absolute maximum bending moment, M_y, increases with increasing thickness/span ratios. This is understandable that increasing the aspect ratio makes the thick plates more flexible in the long span, the y axis, direction. As also seen from this figure, in general, the effects of the changes in the thickness/span ratios on the absolute maximum bending moment, M_y, are larger than the changes in the aspect ratios.

As seen from Fig. 10, the absolute maximum bending moment, M_y, at the center of the thick clamped plates, as in the case of the absolute maximum bending moment, M_y, at the center of the thick simply supported plates, decreases with increasing aspect ratio and increases with increasing thickness/span ratio. The decrease in the absolute maximum bending moment, M_y, increase with increasing aspect ratio. The increase in the absolute maximum bending moment, M_y, increases with increasing thickness/span ratios. This is also understandable that increasing the aspect ratio makes the thick plates more flexible in the long span, the y axis, direction. As also seen from this figure, in general, the effects of the changes in the thickness/span ratios on the absolute maximum bending moment, M_y, are larger than the changes in the aspect ratios.

In this study, the absolute maximum bending moments M_x at the center of the edge in the y direction and the maximum bending moment M_y at the center of the edge in the x direction are not presented for the thick plates clamped along all four edges. It should be noted that the variations of these moments are similar to the absolute maximum bending moments M_x at the center of the thick clamped plates.

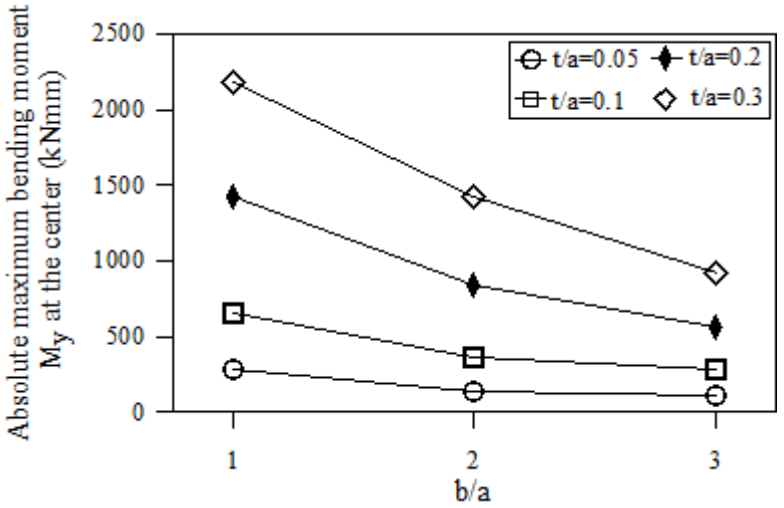

Figure 10. Absolute maximum bending moment M_y at the center of the thick clamped plates resting on Winkler foundation for different aspect ratios and thickness/span ratios.

4. CONCLUSIONS

The purpose of this paper is to study parametric earthquake analysis of thick plates resting on Winkler foundation, to determine the effects of the thickness/span ratio, the aspect ratio and the boundary conditions on the linear responses of the thick plates resting on Winkler foundation subjected to earthquake excitations. It is concluded that 4-noded finite element can be effectively used in the earthquake analysis of thick plates resting on elastic foundation. The coded program can be effectively used in the earthquake analyses of any thick plates resting on elastic foundation. It is also concluded that, in general, the changes in the thickness/span ratio are more effective on the maximum responses considered in this study than the changes in the aspect ratio.

For a thick plates resting on Winkler foundation subjected to the earthquake excitations, it is somewhat difficult to interpret the effects of the thickness/span ratio, the aspect ratio, and the boundary conditions on the responses because both the frequency content of the earthquake excitation and the exact natural frequency of the particular thick plates resting on Winkler foundation can make a difference to its response. In order to generalize the results obtained in this study, the responses of the different thick plates resting on Winkler foundation subjected to different earthquake excitations should be evaluated all together. Therefore, the curves presented herein can help the designer to anticipate the effects of the thickness/span ratio, the aspect ratio, and the boundary conditions on the earthquake response of a thick plate resting on Winkler foundation.

The following conclusions can also be drawn from the results obtained in this study.

The absolute maximum displacements of the thick and thin plates increase as the aspect ratio increases for a constant t/a ratio. The same displacements decrease as the t/a ratio increases for a constant b/a ratio.

The changes in the aspect ratios are generally less effective on the absolute maximum displacement than the changes in the thickness/span ratios.

The absolute maximum bending moment, M_x, at the center of the thick simply supported plates resting on Winkler foundation increases as the aspect ratio and thickness/span ratio increase.

The changes in the aspect ratios are generally more effective on the absolute maximum bending moment, M_x, of the thick and thin simply supported plates than the changes in the thickness/span ratios.

The absolute maximum bending moment, M_x, at the center of the thick clamped plates resting on Winkler foundation increases with increasing aspect ratio and thickness/span ratio.

The changes in the aspect ratios are generally more effective on the absolute maximum bending moment, M_x, of the thick clamped plates resting on Winkler foundation than the changes in the thickness/span ratios.

The absolute maximum bending moment, M_y, at the center of the thick simply supported plates resting on Winkler foundation decreases as the aspect ratio increases and increases as the thickness/span ratio increases.

The changes in the thickness/span ratios are generally more effective on the absolute maximum bending moment, M_y, of the thick simply supported plates resting on Winkler foundation larger than the changes in the aspect ratios.

The absolute maximum bending moment, M_y, at the center of the thick clamped plates resting on Winkler foundation decreases with increasing aspect ratio and increases with increasing thickness/span ratio.

The changes in the thickness/span ratios are generally more effective on the absolute maximum bending moment, M_y, of the thick clamped plates resting on Winkler foundation than the changes in the aspect ratios.

In general, degrees of decreases and increases depend on the changes in the aspect and thickness/span ratios, and the changes in the thickness/span ratio are more effective on the maximum responses considered in this study than the changes in the aspect ratio.

REFERENCES

[1] Winkler, E. (1867), Theory of Elasticity and Strength, Dominicus Pague, Czechoslovakia

[2] Hetenyi, M. (1950), "A general solution for the bending of beams on an elastic foundation of arbitrary continuity." J.Appl. Phys.. 21, 55-58.

[3] Pasternak, PL. (1954) "New method of calculation for flexible substructures on two-parameter elastic foundation". Gasudarstvennoe Izdatelstoo. Literatury po Stroitelstvu I Architekture, 1-56, Moskau.

[4] Vlasov, VZ., Leont'ev, NN. (1989) Beam, plates and shells on elastic foundations. GIFML, Moskau.

[5] Ugural A.C. (1981), *Stresses in Plates and Shells*, McGraw-Hill., New York.

[6] Timoshenko, S. and Woinowsky-Krieger, S. (1959), Theory of Plates and Shells. Second edition, McGraw-Hill., New York.

[7] Leissa A. W. The free vibration of rectangular plates. J Sound Vib 1973; 31 (3): 257-294.

[8] Providakis C. P., Beskos D. E. Free and forced vibrations of plates by boundary elements. Comput Meth Appl Mech Eng 1989;, 74: 231-250.

[9] Qiu J. and Feng Z. C. (2000), "Parameter dependence of the impact dynamics of thin plates," Comput. Struct., 75(5), 491-506.

[10] Grice R. M. and Pinnington R. J. (2002), "Analysis of the flexural vibration of a thin-plate box using a combination of finite element analysis and analytical impedances," J Sound Vib., 249(3), 499-527.

[11] Lok T. S. and Cheng Q. H. (2001), "Free and forced vibration of simply supported, orthotropic sandwich panel," Comput. Struct., 79(3), 301-312.

[12] Si W.J., Lam K. Y. and Gang S. W. (2005), "Vibration analysis of rectangular plates with one or more guided edges via bicubic B-spline method," Shock Vib., 12(5).

[13] Wu L.H. (2012), "Free vibration of arbitrary quadrilateral thick plates with internal colums and uniform elastic edge supports by pb-2 Ritz method," Struct. Eng. Mech., 44(3), 267-288.
[14] Kutlu A., Uğurlu B., Omurtag M.H. (2012), "Dynamic response of Mindlin plates resting on arbitrarily orthotropic Pasternak foundation and partially in contact with fluid", Ocean Eng.. 42, 112-125.
[15] Sheikholeslami S.A., Saidi A.R. (2013), "Vibration analysis of functionally graded rectangular plates resting on elastic foundation using higher-order shear and normal deformable plate theory," Comput. Struct., 106, 350-361.
[16] Senjanovic I.; Tomic M., Hadzic N., Vladimir N. (2017), "Dynamic finite element formulations for moderately thick plate vibrations based on the modified Mindlin theory," Eng. Struct., 136, 100-113.
[17] Tahouneh V. (2014), "Free vibration analysis of thick CGFR annular sector plates resting on elastic foundations," Struct. Eng. Mech., 50(6), 773-796.
[18] Zamani H.A., Aghdam M.M., Sadighi M. (2017), "Free vibration analysis of thick viscoelastic composite plates on visco-Pasternak foundation using higher-order theory," Comput. Struct., 182, 25-35.
[19] Ayvaz Y., Daloğlu A. and Doğangün A. (1998) "Application of a modified Vlasov model to earthquake analysis of the plates resting on elastic foundations," J Sound Vib., 212(3), 499-509.
[20] Omurtag, M.H., and Kadıoğlu, F. (1998), "Free vibration analysis of orthotropic plates resting on Pasternak foundation by mixed finite element formulation," Comput. Struct., 67, 253-265.
[21] Ayvaz Y. and Oguzhan C.B. (2008) "Free vibration analysis of plates resting on elastic foundations using modified Vlasov model.," Struct. Eng. Mech., 28(6), 635-658.
[22] Özgan K., Daloglu A. T. (2012), "Free vibration analysis of thick plates on elastic foundations using modified Vlasov model with higher order finite elements", Int. J. Eng.. Materials Sciences., 19, 279-291.
[23] Zienkiewich O.C., Taylor RL. and Too JM. (1971), "Reduced integration technique in general analysis of plates and shells," Int. J. Numer. Meth. Eng., 3, 275-290.
[24] Zienkiewich O.C., Taylor RL. and Too JM. (1989), The Finite Element Method, fourth ed., McGraw-Hill, New York.
[25] Özdemir Y. I., Bekiroğlu S. and Ayvaz Y. (2007), "Shear locking-free analysis of thick plates using Mindlin's theory," Struct. Eng. Mech., 27(3), 311-331.
[26] Özdemir Y. I., (2012), "Development of a higher order finite element on a Winkler foundation", Finite Elem. Anal.. Des.., 48, 1400-1408.
[27] Özdemir Y. I. (2007), "Parametric Analysis of Thick Plates Subjected to Earthquake Excitations by Using Mindlin's Theory", Ph. D. Thesis, Karadeniz Technical University, Trabzon.
[28] Tedesco J. W., McDougal W. G., Ross C.A. (1999), Structural Dynamics, Addison Wesley Longman Inc., California.
[29] Mindlin, R.D. (1951)," Influence of rotatory inertia and shear on flexural motions of isotropic, elastic plates", J. Appl. M.; 18, 31-38.
[30] Cook, R.D. and Malkus, D.S. and Michael, E.P. (1989), Concepts and Applications of Finite Element Analysis. John Wiley & Sons, Inc., Canada.
[31] Weaver W. and Johnston P. R. (1984), Finite Elements for Structural Analysis, Prentice Hall, Inc., Englewood Cliffs, New Jersey.
[32] Bathe, K.J. (1996), Finite Element Procedures, Prentice Hall, Upper Saddle River, New Jersey.